

Geochemistry, Geophysics, Geosystems

RESEARCH ARTICLE

10.1002/2014GC005588

Key Points:

- Two thermal anomalies may exist within the West Antarctic mantle transition zone
- The West Antarctic mantle transition zone is likely hydrated

Supporting Information:

- Readme
- Supplementary information
- Node_results
- Temp_Anomalies

Correspondence to:

E. L. Emry,
ele11@psu.edu

Citation:

Emry, E. L., A. A. Nyblade, J. Julià, S. Anandakrishnan, R. C. Aster, D. A. Wiens, A. D. Huerta, and T. J. Wilson (2015), The mantle transition zone beneath West Antarctica: Seismic evidence for hydration and thermal upwellings, *Geochem. Geophys. Geosyst.*, 16, 40–58, doi:10.1002/2014GC005588.

Received 26 SEP 2014

Accepted 20 NOV 2014

Accepted article online 26 NOV 2014

Published online 8 JAN 2015

The mantle transition zone beneath West Antarctica: Seismic evidence for hydration and thermal upwellings

E. L. Emry¹, A. A. Nyblade¹, J. Julià², S. Anandakrishnan¹, R. C. Aster³, D. A. Wiens⁴, A. D. Huerta⁵, and T. J. Wilson⁶

¹Department of Geosciences, Pennsylvania State University, University Park, Pennsylvania, USA, ²Departamento de Geofísica e Programa de Pós-Graduação em Geodinâmica e Geofísica, Universidade Federal do Rio Grande do Norte, Natal, Brazil, ³Department of Geosciences, Colorado State University, Fort Collins, Colorado, USA, ⁴Earth and Planetary Sciences, Washington University in St. Louis, St. Louis, Missouri, USA, ⁵Department of Geosciences, Central Washington University, Ellensburg, Washington, USA, ⁶School of Earth Sciences, Ohio State University, Columbus, Ohio, USA

Abstract Although prior work suggests that a mantle plume is associated with Cenozoic rifting and volcanism in West Antarctica, the existence of a plume remains conjectural. Here we use *P* wave receiver functions (PRFs) from the Antarctic POLENET array to estimate mantle transition zone thickness, which is sensitive to temperature perturbations, throughout previously unstudied parts of West Antarctica. We obtain over 8000 high-quality PRFs using an iterative, time domain deconvolution method filtered with a Gaussian width of 0.5 and 1.0, corresponding to frequencies less than \sim 0.24 and \sim 0.48 Hz, respectively. Single-station and common conversion point stacks, migrated to depth using the AK135 velocity model, indicate that mantle transition zone thickness throughout most of West Antarctica does not differ significantly from the global average, except in two locations; one small region exhibits a vertically thinned (210 ± 15 km) transition zone beneath the Ruppert Coast of Marie Byrd Land and another laterally broader region shows slight, vertical thinning (225 ± 25 km) beneath the Bentley Subglacial Trench. We also observe the 520 discontinuity and a prominent negative peak above the mantle transition zone throughout much of West Antarctica. These results suggest that the mantle transition zone may be hotter than average in two places, possibly due to upwelling from the lower mantle, but not broadly across West Antarctica. Furthermore, we propose that the transition zone may be hydrated due to >100 million years of subduction beneath the region during the early Mesozoic.

1. Introduction

The mantle transition zone is characterized by mineral phase transitions that occur from depths of \sim 410 to \sim 660 km. For the olivine-normative component of the mantle, those include olivine (α -spinel) to wadsleyite (β -spinel) at 410 km, wadsleyite (β -spinel) to ringwoodite (γ -spinel) at 520 km, and ringwoodite (γ -spinel) to perovskite at 660 km [Bina and Hellfrich, 1994]; for the pyroxene-normative component, phase transitions from majoritic garnet to perovskite are also expected near 660 km depth. Phase transitions in the olivine component create relatively sharp jumps in seismic velocity (discontinuities) that produce *P*-to-*S* conversions in *P* wave receiver functions (PRFs) that can be distinguished from noise, commonly after stacking tens to hundreds of traces arising from diverse, distant earthquake sources [Langston, 1979; Shearer, 1991; Dueker and Sheehan, 1997]. A phase transition in the pyroxene component is less likely to be identified, due to the broad depth over which the transition occurs [e.g., Weidner and Wang, 2000]. Because the 410 and 660 km phase transitions possess opposite Clapeyron slopes (dP/dT), transition zone thickness should vary with lateral changes in temperature. In regions where the transition zone is hot, as would be expected for a mantle upwelling, the transition zone is expected to thin [Bina and Hellfrich, 1994]. Observations from receiver functions and SS-precursors give a global average transition zone thickness of \sim 240–260 km [Shearer, 1991; Chevrot et al., 1999; Lawrence and Shearer, 2006].

The presence of other discontinuities or velocity structure within or in close proximity to the mantle transition zone may reflect thermal and/or chemical anomalies, and steady improvement in seismic coverage has driven more widespread and detailed studies of finer-scale structure. A region of low velocity above the mantle transition zone has been detected beneath a number of locations, including at the South Pole (SPA) and Dumont d'Urville (DRV) stations in Antarctica [Vinnik and Farra 2007, and

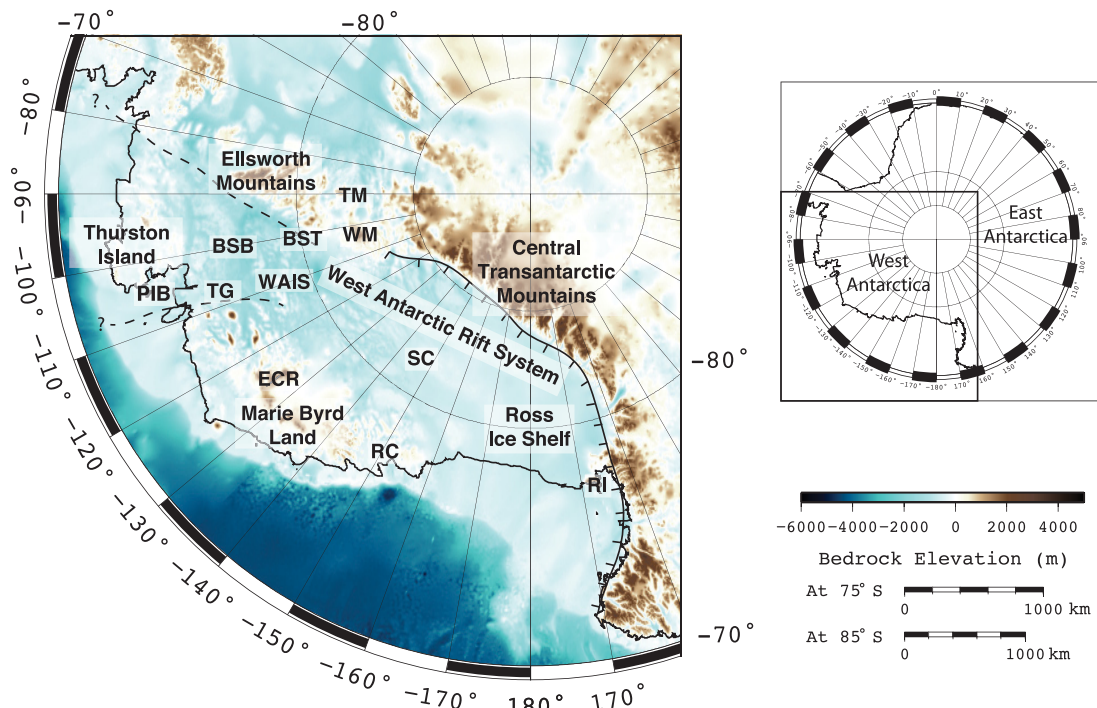


Figure 1. Topographic and bathymetric map of all of West Antarctica, including western Ross Ice Shelf and Ross Island, from BEDMAP2 [Fretwell et al., 2013]. Names of major geographic regions are given; minor geographic features and locations are given acronyms as follows: BSB, Byrd Subglacial Basin; BST, Bentley Subglacial Trench; ECR, Executive Committee Range; PIB, Pine Island Bay; RC, Ruppert Coast; RI, Ross Island; SC, Siple Coast; TG, Thwaites Glacier; TM, Thiel Mountains; WAIS, West Antarctic Ice Sheet Divide Field Station; WM, Whitmore Mountains. Black line with perpendicular hatches indicates the trace of the West Antarctic Rift System that is well known, and dashed black lines indicate possible eastward or northward extension of the rift [Jordan et al., 2010].

references therein]. Revenaugh and Sipkin [1994] proposed that the negative peak is indicative of dense partial melts above the 410 km phase transition and Bercovici and Karato [2003] hypothesized that partial melting could be induced by upward migration of hydrous transition zone material. Similarly, decreased seismic velocity below the 660 km discontinuity in mantle downwelling regions below western North America has been inferred as arising from hydrated ringwoodite transitioning to perovskite with partial melt [Schmandt et al., 2014]. The 520 km discontinuity is also frequently observed, and it is proposed that variability in its characteristics (presence or absence, depth, splitting, amplitude, and breadth) reveals information about regional differences in the composition (fertile mantle or depleted subducted slabs; water-rich or dry) and temperature of transition zone materials [e.g., Ita and Stixrude, 1992; Weidner and Wang, 2000; Deuss and Woodhouse, 2001; Saikia et al., 2008]. Furthermore, a deep discontinuity around 720 km has been interpreted as evidence for hotter than average material at the base of the transition zone, caused by the shifting of the phase transition in the garnet majorite component of the mantle due to its positive Clapeyron slope [Simmons and Gurrola, 2000; Andrews and Deuss, 2008; Yu et al., 2011]; complicated receiver function peaks corresponding to the base of the transition zone have been detected globally at a number of locations, including beneath the Erebus hot spot [Andrews and Deuss, 2008].

West Antarctica is comprised of several distinct provinces that began to rift apart during the Cretaceous as the West Antarctic Rift System formed (Figure 1) [Dalziel and Elliot, 1982; Grunow et al., 1991; Dalziel, 1992]. The timing and development of rifting throughout the region is not well constrained due to lack of geological and geophysical data; however, evidence from fission track dates from the Transantarctic Mountains, which are thought to have formed due to rift-flank uplift, indicates multiple stages of uplift and denudation [Stump and Fitzgerald, 1992]. In some continental rifts (e.g., East Africa), extensional development may be aided or initiated by deep thermal mantle upwellings [e.g., Hansen and Nyblade, 2013; Mulibbo and Nyblade, 2013]. Several petrological and geochemical studies suggest that the volcanics of West Antarctica, in

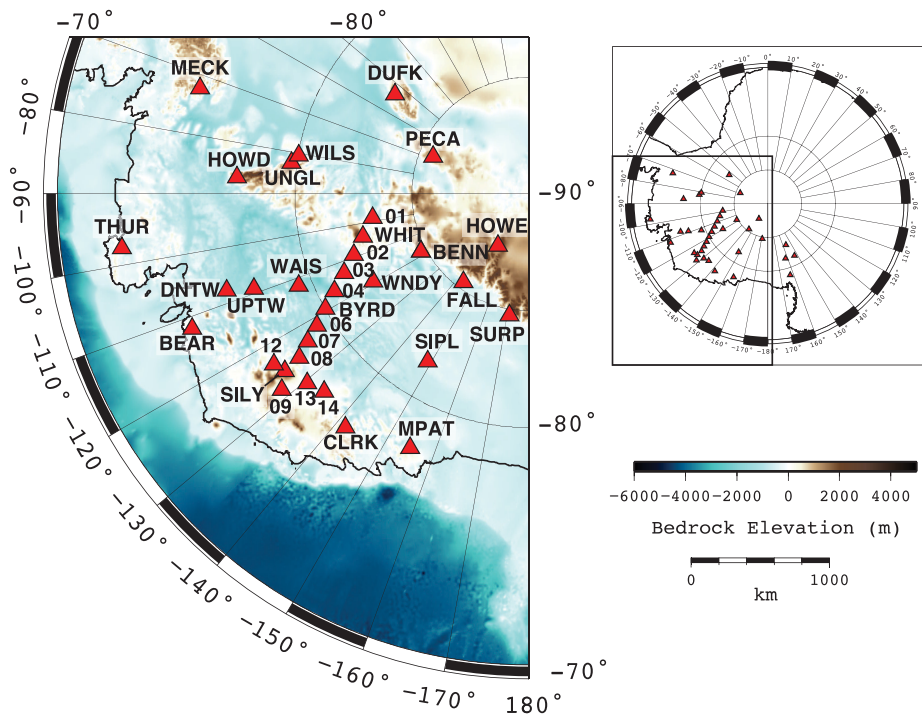


Figure 2. Map of ANET seismic stations in West Antarctica used in this study (red triangles). The 2010–2012 ANET transect stations are denoted only by number (full station code is ST01, ST02, etc), and the backbone stations (the rest of the ANET array) are marked with their full station codes.

particular around Marie Byrd Land, are likely derived from a deep mantle source, although interpretations vary [e.g., Panter *et al.*, 1997, 2000; Kipf *et al.*, 2014].

Seismic velocities within the upper mantle beneath West Antarctica are distinctly slower than the average upper mantle ($\sim 0.5\text{--}1\%$ V_p ; $\sim 3\text{--}5\%$ V_s); a number of continental-scale tomography studies identify one or multiple low-velocity regions that appear to stretch downward through the upper mantle as would be expected for a thermal upwelling rising from the lower mantle [e.g., Sieminski *et al.*, 2003; Morelli and Danesi, 2004; Hansen *et al.*, 2014]. However, regional tomographic modeling beneath the Erebus hot spot region of West Antarctica indicates a low-velocity anomaly within the upper mantle that reaches to 300–400 km depth, but does not extend into the transition zone [Watson *et al.*, 2006]. A P wave receiver function study of the same region found that the transition zone thickness is not significantly different from the global average of $\sim 240\text{--}260$ km, further indicating that the Erebus anomaly is confined to the upper mantle [Reusch *et al.*, 2008].

Recent regional seismic tomography images covering parts of West Antarctica, including Marie Byrd Land, the Byrd Subglacial Basin, and the Ellsworth and Whitmore Mountains corroborate what is observed in continental-scale tomography, imaging slow seismic velocities extending through the upper mantle and possibly also into the mantle transition zone [Heeszel, 2011; Lloyd *et al.*, 2013; Hansen *et al.*, 2014]. However, because the surface wave tomographic model of Heeszel [2011] is limited to upper mantle depths ($\sim <250$ km), and body wave tomography models tend to have large vertical smearing ($\sim 100\text{--}200$ km) and decreased resolution at mantle transition zone depths [Lloyd *et al.*, 2013; Hansen *et al.*, 2014], the extent to which rifting and volcanism in these parts of West Antarctica has been affected by mantle thermal upwellings, originating within or below the transition zone, remains unclear (see discussion in supporting information).

To determine whether the mantle transition zone beneath regions of West Antarctica, excluding the previously studied Erebus hot spot region, shows evidence for a deep thermal anomaly, we analyzed PRFs from stations within the ongoing Antarctic POLENET (ANET) seismic deployment (Figure 2) that are located in the vicinity of Marie Byrd Land, the Central Transantarctic Mountains, the Ellsworth-Whitmore Mountains, and the Byrd Subglacial Basin.

2. Background

2.1. Antarctic Tectonics and Volcanism

From 230 to 125 Ma, West Antarctica is thought to have been comprised of four blocks—Thurston Island, Marie Byrd Land, South New Zealand, and the Antarctic Peninsula—and was bordered along most of its length by subduction zones. Progressively, subduction ceased along the margin [Dalziel, 1992]. Around 90 Ma, West Antarctica began to rift, separating the South New Zealand block from the rest of the landmass [Dalziel and Elliot, 1982; Grunow et al., 1991; Dalziel, 1992]. The Transantarctic Mountains along the southern flank of the rift were uplifted in multiple phases at ~110, ~80, and ~60 Ma [Stump and Fitzgerald, 1992]. The low current rates of seismicity and deformation throughout West Antarctica suggest that rifting is presently very slow or inactive [Winberry and Anandakrishnan, 2003].

About 30 subaerial volcanoes occur throughout West Antarctica, and geophysical surveys of the subsurface beneath the West Antarctic Ice Sheet have identified numerous subglacial volcanoes [Behrendt et al., 1991; Blenkinsop et al., 1993; Behrendt, 2012; Lough et al., 2013]. Many of the volcanoes located in Marie Byrd Land are geochemically similar to oceanic island basalts (OIB), but the region as a whole differs from the OIB paradigm because of the abundance of felsic rocks as well [LeMasurier, 1990]. Although none of the basaltic volcanoes in Marie Byrd Land demonstrate an age progression, several of the intermediate-felsic composition volcanic ranges exhibit spatially variable linear age progressions that are not aligned to hot spot reference frame plate motions but may be structurally controlled and/or influenced by small-scale convection [e.g., LeMasurier and Rex, 1989; LeMasurier, 1990; van Wijk et al., 2010]. Deep low-frequency seismicity and ash layers within the West Antarctic Ice Sheet further demonstrate the ongoing volcanic nature of the region [Behrendt, 2012; Lough et al., 2013]. In addition to the prevalence of volcanic rocks throughout Marie Byrd Land, notably high heat fluxes have been observed beneath portions of the West Antarctic Ice Sheet [Alley and Bentley, 1988; Clow et al., 2012].

The source for the varied compositions and distribution of West Antarctica volcanoes and adjacent seamounts is still debated; several models have been proposed to explain their existence and observed patterns, including a broad upper mantle hot spot [LeMasurier and Rex, 1989], a large thermal mantle plume [e.g., LeMasurier and Landis, 1996], two distinct thermal mantle plumes—one beneath Erebus and one beneath Marie Byrd Land [e.g., Storey et al., 1999], upwelling upper mantle triggered by catastrophic detachment of a subducting plate [Finn et al., 2005], and reactivation of plume material accreted to the base of the lithosphere during the Cretaceous [Kipf et al., 2014].

2.2. The Structure of the Mantle Beneath West Antarctica

Continent-wide surface wave tomography images using sparse long-running seismographic stations clearly demonstrate that the upper mantle of West Antarctica is distinctly slower than East Antarctica and that broad low velocities within the West Antarctic upper mantle persist to at least ~200 km depth. However, for many of these models, the lateral resolution ranges from ~200 to 700 km [Ritzwoller et al., 2001; Danesi and Morelli, 2001; Sieminski et al., 2003; Morelli and Danesi, 2004]. A global model using higher-mode surface wave tomography to solve for hydration and temperature within the mantle transition zone suggests that the broad region of West Antarctica is about 25–50°C warmer with ~0.25 wt % more H₂O than the mean global average [Meier et al., 2009]. Prior to ANET, detailed regional studies were carried out near the Erebus hot spot beneath the western edge of the Ross Ice Shelf. Results image an abrupt lateral boundary between the slower and warmer upper mantle of West Antarctica and the faster and colder upper mantle of East Antarctica [Watson et al., 2006; Lawrence et al., 2006]. Despite the differences in upper mantle velocities, results from a prior PRF study beneath this region identified no thinning of the mantle transition zone, suggesting that the slow velocities beneath the Erebus region are confined to the upper mantle [Reusch et al., 2008]. Recent tomographic results from Hansen et al. [2014] also suggest that the transition zone beneath the Erebus hot spot is not thermally perturbed, but do indicate that portions of the mantle transition zone beneath Marie Byrd Land could be hotter than average.

3. Methods

3.1. The Antarctic POLENET Deployment

Seismic data from the ANET deployment consist of an ongoing “backbone” network that began collecting data in 2007, including a temporary seismic transect that collected data from 2010 to 2012 (Figure 2). The transect crosses the West Antarctic rift from the coast of eastern Marie Byrd Land, near the Executive

Committee Range over the Byrd Subglacial Basin and Bentley Subglacial Trough, and into the Whitmore Mountains. The backbone ANET stations are equipped with cold-rated broadband seismic stations (Guralp CMG-3T or Nanometrics Trillium-240 with Quanterra Q330 data loggers) and an associated constellation of GPS receivers [Anthony *et al.*, 2015] (polenet.org; passcal.nmt.edu; unavco.org). The transect stations were equipped with broadband seismometers only.

3.2. Data Selection and Receiver Function Deconvolution

We calculated PRFs from ANET seismographs that were located east of the Ross Ice Shelf. The data selection and preprocessing follows the approach detailed within *Julia and Nyblade* [2013] and is briefly summarized here. Seismic sources at epicentral distances ranging from 30° to 90° from the recording stations were selected and the corresponding waveforms were cut 10 s before and 100 s after the theoretical arrival of the teleseismic P wave. The waveforms were demeaned, detrended, and tapered using a 5% cosine window and high-pass filtered above 0.05 Hz to remove long-period instrumental noise. The filtered traces were resampled at 20 samples per second, after low-pass filtering at 8 Hz to avoid aliasing. The horizontal components were then rotated into the great circle path to obtain the radial and transverse components, and the vertical component was deconvolved from the corresponding horizontal components to obtain the radial and transverse receiver functions using the iterative, time domain deconvolution method of *Ligorria and Ammon* [1999], with 500 iterations. During the deconvolution, we used Gaussian filter widths of 0.5 and 1.0, corresponding to frequencies of less than ~ 0.24 and ~ 0.5 Hz, respectively. The specific filters were chosen to remove high-frequency noise while exploring the sharpness and reliability of detected peaks.

We evaluated the quality of the deconvolution by convolving the vertical component back with the final radial receiver function, automatically rejecting all receiver functions that did not recover at least 80% of the original radial waveform. We further refined the data set by identifying events with unusually large amplitudes on the transverse receiver functions and removing the corresponding radial receiver function, as this could indicate difficulties during the rotation process. Additionally, we removed all radial receiver functions with large amplitudes, above a threshold value (0.12–0.15), from the data set. We do this to ensure that large amplitude noise levels on horizontal components—as documented at a few of the seismic stations—do not impact the final stacks for each station [Anthony *et al.*, 2015].

Finally, we visually inspected the radial receiver functions, comparing each with several others, to identify and remove noticeable outliers. We identified outliers by large negative amplitudes, harmonic oscillations, comparatively small direct arrival peaks, or subdued crustal Ps peaks [e.g., Benoit *et al.*, 2013]. For the stations where only 1 year of data were collected, this stage of the quality check significantly increased confidence in detected peaks. To limit subjectivity from this step, we did not identify traces with positive peaks at times corresponding to where we expect the 410 and 660 discontinuities. The initial number of events and the final number of quality receiver functions in each single-station stack are included in the supplementary material (Table S1). On average, we obtained quality receiver functions from ~ 15 to 25% of the available events, although for a small number of stations only ~ 5 –10% of the available events were of sufficient quality.

3.3. Migration and Stacking

We migrated and stacked radial receiver functions for each station using the common conversion point stacking method [Owens *et al.*, 2000]. Assuming a 1-D velocity model (AK135), we computed the theoretical latitude and longitude (piercing points) of an incoming ray at 5 km depth intervals, extending from the surface to 800 km [Kennett *et al.*, 1995; Crotwell *et al.*, 1999]. The piercing points were then grouped into bins of a specified radius around predefined nodes and the PRF amplitudes corresponding to the theoretical Ps-P travel-times associated with each pierce point were averaged. The receiver function amplitudes between the depth-migrated points were then linearly interpolated.

Using the Owens *et al.* [2000] methodology, incoming rays that do not fall within a specified bin radius around each station (or latitude/longitude node) were excluded from the stack. For single-station stacks throughout West Antarctica, we set a single node at the station location and a bin radius of 5° along a great circle arc, which provides sufficient distance to incorporate all high-quality PRFs for the station. For all

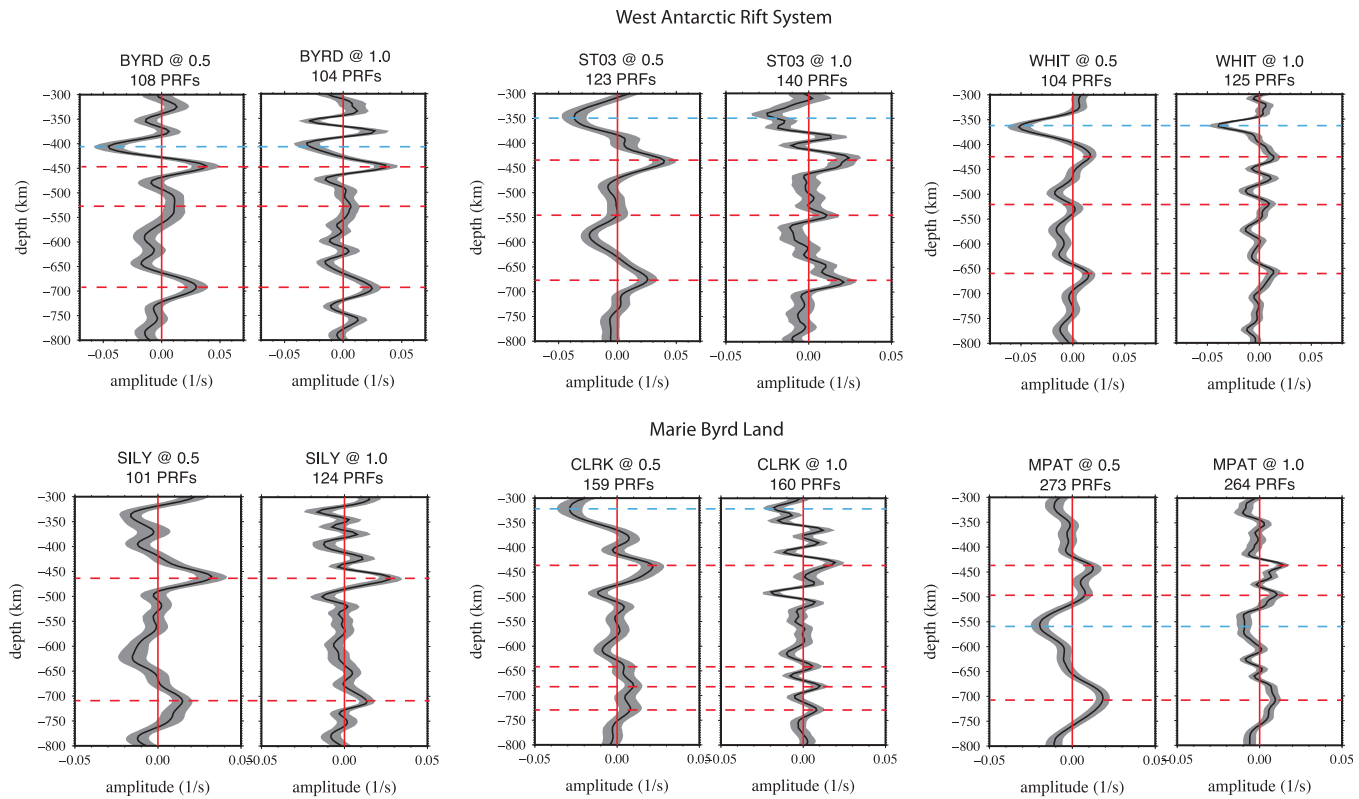


Figure 3. Select single-station receiver function (PRF) stacks are plotted for ANET stations in Marie Byrd Land and the West Antarctic Rift. For each station, PRFs are filtered with a 0.5 and 1.0 Gaussian width filter; number of PRFs in the stack is noted. The 95% confidence bounds are shown (gray) behind the full stack (black line). Positive peaks are marked with a dashed red line; negative peaks are noted with dashed blue line. At stations where multiple prominent peaks are present (i.e., CLRK and MPAT stations), all peaks are marked with dashed red line.

stacks, confidence bounds are computed from the set of quality receiver functions by bootstrap resampling [Efron and Tibshirani, 1991]. Examples of several single-station stacks are shown in Figure 3.

We next tested the effects of velocity model variability on the receiver function depth migration and consequent transition zone thickness. Recent tomographic results show velocity decreases of \sim 1–2% in Vp [Lloyd et al., 2013; Hansen et al., 2014] and \sim 3–5% in Vs [Heeszel, 2011] in the region beneath Mount Sidley in Marie Byrd Land. We created several 1-D velocity models, varying upper mantle and transition zone Vp/Vs ratios consistent with the above degree of variability, and then migrated and stacked the receiver functions at the West Antarctic Ice Sheet (WAIS) Divide seismic station; for each test, we note the resultant stacked discontinuity depths and transition zone thickness (Tables S2 and S3). We conclude that, at most, 5–10 km of variation in inferred transition zone thickness could be unaccounted for by velocity variations consistent with recent tomography models. A more thorough description of these tests and the resolutions of recent tomography results are found in supporting information (Tables S2–S4 and Figures S1–S3).

3.3.1. Common-Conversion Point Stacking

Good ray coverage, as evidenced by pierce point (conversion point) plots due to the spatially dense transect stations, allowed us to stack data from multiple stations sampling the transition zone at a given location (Figure 4), thus increasing our resolution of mantle transition zone structure throughout much of West Antarctica. We used the common conversion point stacking method of Owens et al. [2000], combining all of the stations located throughout the region, and then stacking all of the receiver functions that fall within a specified radius around each nodal point at each depth increment. Because the distance between longitudinal degrees decreases as latitude decreases (from \sim 33 km at -72.5° to \sim 10 km at -85°), we vary the spacing of our nodal points throughout the region (5° longitude between nodes at -75°N to -80°N ; 10° longitude between nodes at -80°N to -85°N) to eliminate geographic distortion. We allow in each stack

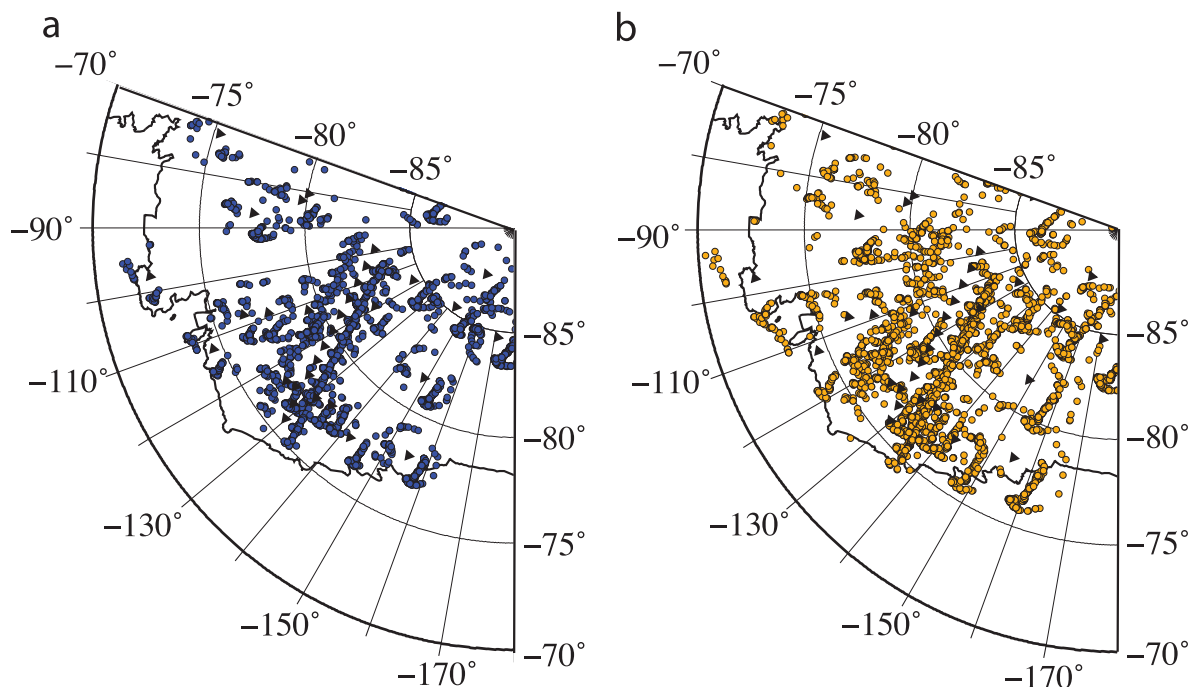


Figure 4. Map of Ps conversion points at (a) 410 km and (b) 660 km depth beneath West Antarctica. The blue and orange circles designate the location of incoming rays at 410 and 660 km depth, respectively, corresponding to each individual, high-quality receiver function. Only individual receiver functions that were used to create single-station and common conversion point stacks are shown; no rejected conversion points are plotted. The black triangles show the locations of the seismic stations (Figure 2).

all incoming rays within 1.25° and 1.5° of the nodal point (equivalent to ~ 135 and ~ 165 km at the equator). This provides overlap in the incoming energy contributing to the stacks at each station, similar to a running average. On each nodal stack, the set of receiver functions are resampled (as discussed above), and a depth error is estimated from the higher-frequency data, where the amplitudes of the peaks are above zero (Table 1; supporting information Table) [Abt *et al.*, 2010]. Figure 5 demonstrates our corresponding error determinations.

4. Results

We rejected (did not interpret) all stack peaks for which at least one of the following criteria apply: less than 50 receiver functions were available, the stack was noisy (many large amplitude peaks), or the lower confidence bound (95% confidence level) was not above zero amplitude. The final interpreted peaks described below, plotted in Figures 6–9, listed in Table 1, and provided in the supporting information, exceeded these criteria. In Figures 6–9, we show that although high-quality receiver functions are located throughout West Antarctica, there are some places in the studied region where not enough quality data existed to make a robust interpretation of the stacks. Our overlapping bins are averaged using the nearest neighbor gridding method (Figures 6–9); unlike other gridding methods, the nearest neighbor method creates weighted averages for only regions of bin overlap based on proximity to the center of the contributing bin. Nearest neighbor averaging does not extrapolate into regions far outside of where our interpreted stacks exist, thereby limiting the spatial extent of our interpretations only to the region immediately surrounding the prescribed nodal location (www.soest.hawaii.edu/gmt/).

4.1. Topography of the 410 km Discontinuity

As Figure 6 demonstrates, nearly all of the studied area exhibits a depressed 410 discontinuity. Where the transition zone is of average thickness, a depressed 410 discontinuity implies that the actual olivine-wadsleyite (410) phase transition depth is not different than for the average Earth (as would be expected for a thermally altered transition zone), but rather the apparent downward shift of the transition zone is an

Table 1. Selected Results of CCP Stacking^a

Node Location ^b		410 Discontinuity Depth (km) ^c		660 Discontinuity Depth (km) ^c		Transition Zone Thickness (km)	
Latitude (°N)	Longitude (°E)	gw ^d = 0.5	gw = 1.0	gw = 0.5	gw = 1.0	gw = 0.5	gw = 1.0
-76.00	-150.00	440 ± 14.2 21.7	430 ± 7 4.4	645 ± 14.3 83.8	640 ± 6.2 6.6	205	210
-80.95	-110.00	440 ± 11.1 17.4	430 ± 6.9 31.0	665 ± 13.7 17.3	655 ± 11.4 38.1	225	225
-80.95	-120.00	445 ± 12.1 9.2	445 ± 6.5 6.9	670 ± 16.5 14.8	670 ± 18.9 18	225	225
-80.95	-130.00	440 ± 9.7 15.1	445 ± 6.3 7.4	670 ± 13.1 14.4	675 ± 20 11.7	230	230
-82.30	-100.00	440 ± 18.3 14.3	430 ± 12.6 22.2	660 ± 13 22.5	650 ± 11.1 53.4	220	220
-82.30	-110.00	430 ± 15.4 42.6	425 ± 6.5 11.4	665 ± 15.9 10.4	660 ± 12.6 12	235	235
-82.30	-120.00	440 ± 17.2 14.5	435 ± 7.1 11.6	665 ± 10.8 11.5	665 ± 11.8 11.1	225	230

^aValues correspond to a bin radius of 1.5°, highlighted in bold in supporting information.^bLocation of nodes given in table corresponds to the anomalies beneath the Ruppert Coast (RC) in line 1 and the Bentley Subglacial Trench/Whitmore Mountains region (BST/WM) in lines 2–7.^cDepth errors are calculated as distance (km) to the upper (top number) and lower (bottom number) uncertainty bounds (determined by bootstrap resampling) at the amplitude of the full stack peak.^dThe Gaussian width of the filter.

effect of upper mantle structure. Topographic variation of the 410 discontinuity is useful to indicate, geographically, where the largest upper mantle anomalies might exist. Throughout the region, the 410 discontinuity is depressed by 20–60 km. We find the most pronounced depression of the 410 (without corresponding thinning of mantle transition zone) beneath the Executive Committee Range in Marie Byrd Land and in the vicinity of the Thwaites Glacier and Pine Island Bay, where the 410 is depressed by 50–60 km (Figure 6).

4.2. Mantle Transition Zone Thickness

Although the 410 discontinuity is depressed throughout much of West Antarctica, transition zone thickness is not significantly different from the global average of 240–260 km (Figure 7). Two regions show very slight thickening, one beneath WAIS Divide/Thwaites Glacier and the other beneath a portion of western Marie Byrd Land; however, in both of these locations, the transition zone is only ~10–20 km thicker than the global average, with somewhat large vertical uncertainties (see supporting information). Thinning of the transition zone is found below the Ruppert Coast, where the transition zone thins to 210 ± 15 km, and the Bentley Subglacial Trench, where the transition zone is 225 ± 25 km thick (Figures 5 and 7, Table 1, and supporting information). Vertical uncertainties given above and discussed throughout the paper are upward-rounded estimates based on the sum of ε_{410u} and ε_{660d} from stacks with the best-resolved peaks, i.e., generally higher-frequency stacks (Figure 5, Table 1, and supporting information).

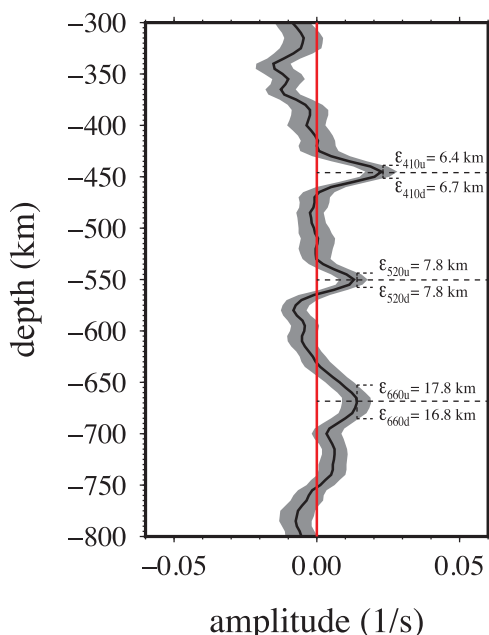


Figure 5. Example PRF from the node located at 80.95°S, 120°W for Gaussian width 1.0 and bin radius of 1.25° (Figure 7c) showing how vertical errors are determined from bootstrap confidence bounds. Vertical errors are determined as the distance from the full stack peak amplitude to the upper and lower bound depth, at the same amplitude as the full stack peak.

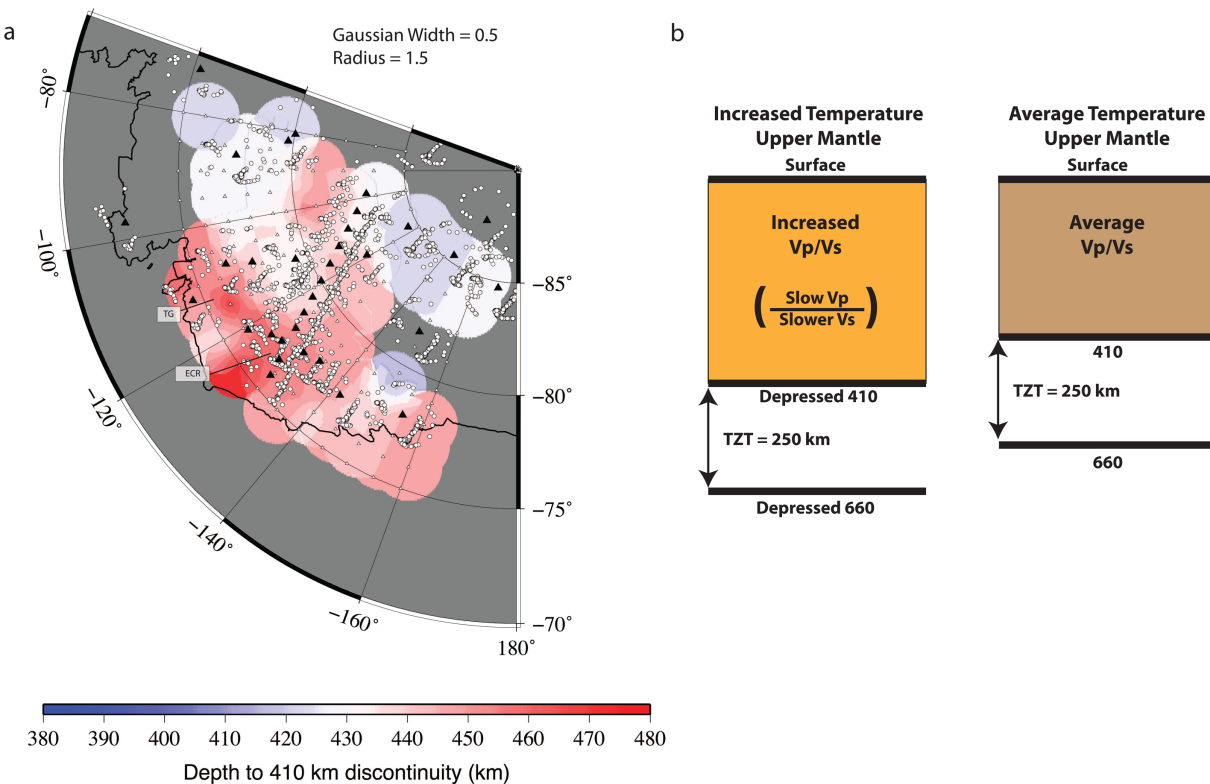


Figure 6. (a) Map showing the depth of the 410 discontinuity for a 1.5° bin radius and a Gaussian filter width of 0.5 for nodes with quality peaks that were deemed to be robust. The map is created with the nearest neighbor averaging function in GMT to specify the bin radius and average transition zone thicknesses where stacks overlap laterally (<http://www.soest.hawaii.edu/gmt/>). Black triangles show station locations, and small circles are the Ps conversion points for high-quality individual receiver functions that were used in the final stacks. (b) Diagram demonstrating the significance of (apparent) depressed 410 discontinuity given no significant changes in transition zone thickness (TZT), as discussed in the main text (sections 4.1 and 5.3).

Beneath the Ruppert Coast, indications for complicated transition zone structure are apparent at two stations, Mt. Clark (CLRK) and Mt. Paterson (MPAT). These seismographs have collected 3+ years of data and have experienced no major temporal recording gaps [Anthony et al., 2015]. Both are located on rock or in the snow above shallow bedrock. As seen in Figure 3, both CLRK and MPAT single-station stacks have complicated lower peaks, either broad (MPAT) or exhibiting multiple lower peaks (CLRK). We suggest that this is a result of laterally varying transition zone thickness that is averaged together in the single-station stacks. When common conversion point stacking is employed, the largest peak corresponding to the base of the transition zone shifts upward and is the shallowest beneath the Ruppert Coast of the Ross Sea (near 76°S , 150°W) (Figure 7d). Several seismographs were located in the vicinity of the Bentley Subglacial Trench, which was a target of the 2010–2012 transect. Most of this region (Figure 7c) has \sim 100–400 individual quality receiver functions within each stacked depth, although the amount of data in each stack decreases toward the east beneath the Thiel and Ellsworth Mountains (\sim 50–100 RFs).

4.3. 520 Discontinuity

Throughout much of the study region, a low-amplitude positive peak at \sim 480–550 km depth is resolved, and we interpret these peaks as the 520 discontinuity (Figures 3, 5, 7c, and 8). As expected, these peaks tend to be smaller in amplitude than the 410 and 660 discontinuities (Figure 8b). In many places, although the full stack shows a peak above zero amplitude, the lower confidence bound is below zero amplitude; in these instances, no peak is interpreted. Because the 520 is a weaker amplitude peak and because it was detected nearly everywhere where numerous traces were collected, its absence may be due to transition zone properties or could be a result of incomplete coverage. In several of the stacks near the Central

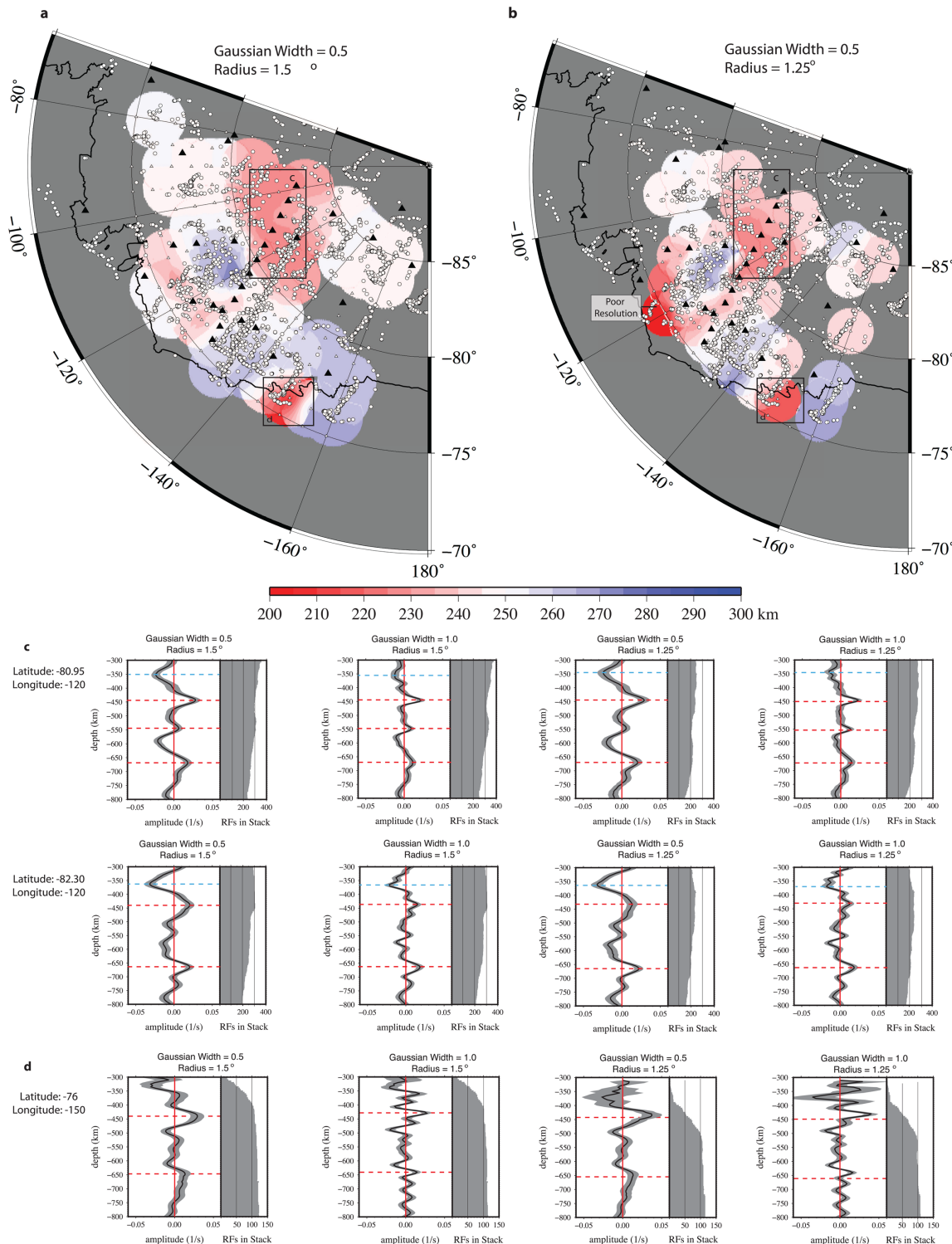


Figure 7. Maps of West Antarctica showing mantle transition zone thickness for nodes with quality 410 and 660 peaks. Black triangles show station locations and small circles are the Ps conversion points for high-quality individual receiver functions that were used in the final stacks. (a) Transition zone thicknesses identified from stacks with 1.5° bin radius and a Gaussian filter width of 0.5. (b) Transition zone thicknesses identified from stacks with a 1.25° bin radius and a Gaussian filter width of 0.5. (c) Selected stacks (multiple filters and bin radii) at nodes located near the Bentley Subglacial Trench (BST) and Whitmore Mountains (WM) regions. Histograms demonstrating the number of individual PRFs contributing to the stack at each depth are shown on the right of each receiver function stack. (d) Same as in Figure 7c, but for the node located at the Ruppert Coast of Marie Byrd Land. Values for the transition zone thicknesses at several of the nodes within boxes c and d are given in Table 1.

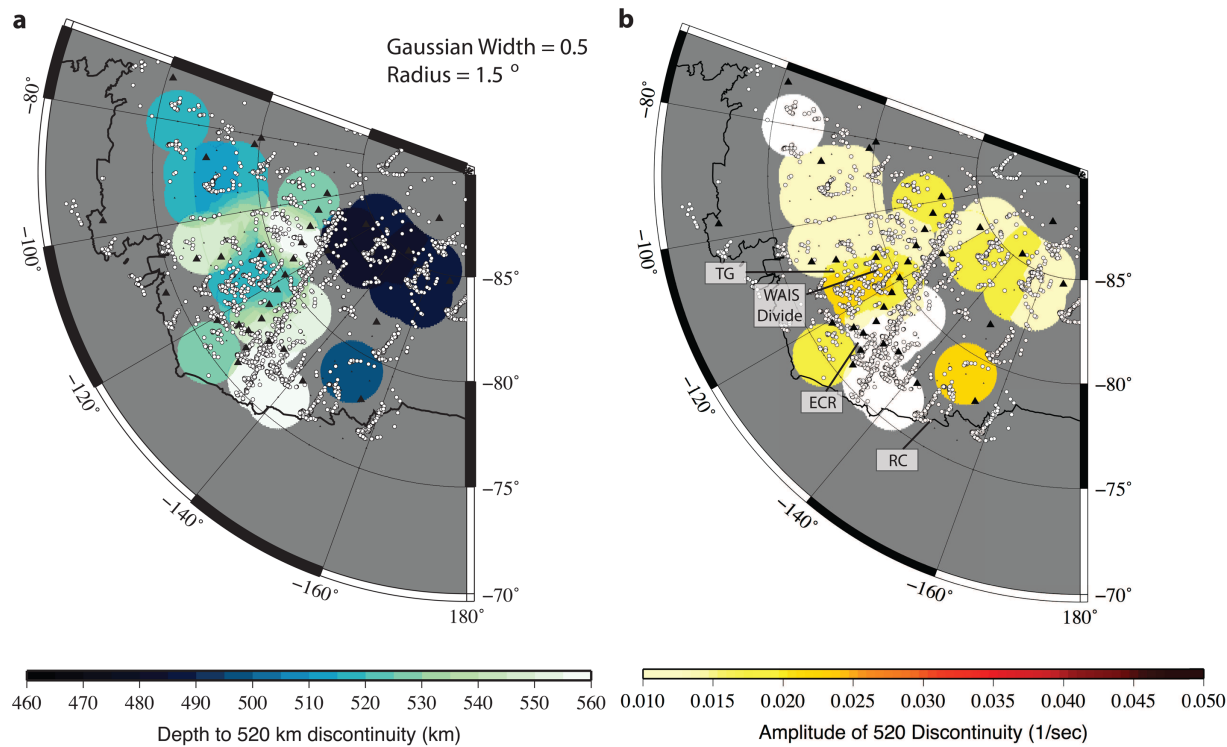


Figure 8. (a) Map showing the depth (km) of the 520 discontinuity for a 1.5° bin radius with a Gaussian filter width of 0.5 for nodes with quality peaks. (b) Map showing the amplitude of the 520 discontinuity for a 1.5° bin radius with a Gaussian filter width of 0.5. Black triangles show station locations, and small circles are the Ps conversion points for high-quality individual receiver functions that were used in the final stacks.

Transantarctic Mountains, a very shallow peak at ~ 480 km is observed (Figure 8), and in some stacks, a second, deeper positive peak is also detected. Detailed results for location, depth, and amplitude of the 520 are given in supporting information.

4.4. Negative Peaks Above 410

Throughout much of West Antarctica, a prominent negative peak is detected above the transition zone (Figures 3, 7, and 9). The negative peak is located at ~ 350 – 400 km depth throughout the West Antarctic region and generally corresponds to the variations of the 410 discontinuity, although it appears to shallow significantly (~ 330 km depth) in the western portions of our study region beneath western Marie Byrd Land and the Central Transantarctic Mountains (Figure 9). The strongest amplitude (negative) peak was located beneath the Bentley Subglacial Trench, the Byrd Subglacial Basin, and the Ellsworth Mountains. We interpret only the peaks for which the upper error bound is distinctly below the zero amplitude line and the stacked negative amplitude is in the range of ~ 0.02 – 0.05 —which is roughly equal to the magnitude of the 410 and 660 peak amplitudes and noticeably more pronounced than the 520 discontinuity (Figures 8 and 9).

4.5. Sub-660 Discontinuity (720)

In several regions, multiple positive peaks are recorded either on the upper or the lower boundary of the transition zone (Figures 3 and 7), as has been observed before for global transition zone receiver function studies [Andrews and Deuss, 2008]. Although possible low-amplitude negative peaks below the 660 discontinuity may exist on some of the stacks (Figures 3, 5, and 7), they are not prominent features; and so unlike Schmandt *et al.* [2014], we do not see an obvious indication for transient partial melt below the 660. In particular, observed complexity of the 660 discontinuity appears on the CLRK single stack and for the stack beneath the Ruppert Coast (Figure 7d). Beneath the Bentley subglacial trench and Whitmore Mountains, evidence for multiples and/or asymmetry exists on several of the stacks (Figure 7c). However in these cases, the upper peak is also complex, with a broad upper

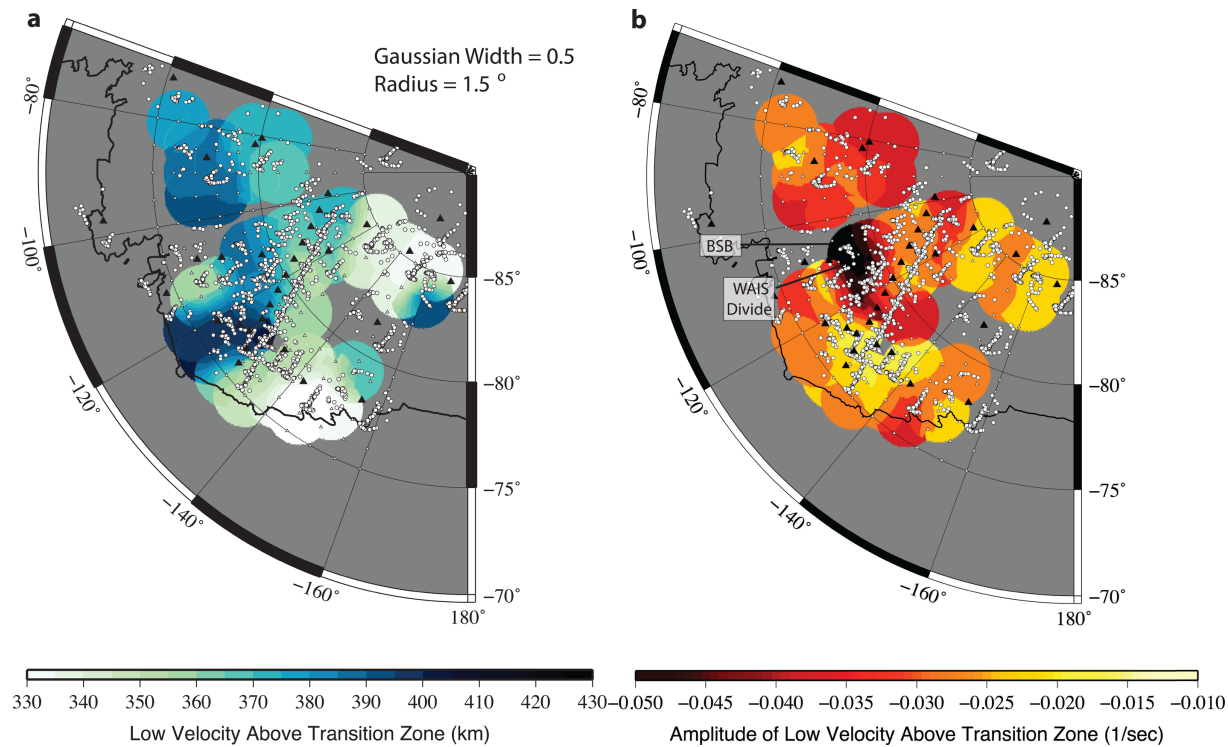


Figure 9. (a) Map showing the depth (km) of negative peaks above the transition zone for a 1.5° bin radius and a Gaussian filter width of 0.5 for nodes with quality peaks. (b) Map showing the amplitude (1/s) of negative peaks above the transition zone for a 1.5° bin radius with a Gaussian width of 0.5. Black triangles show station locations, and small circles are the Ps conversion points for high-quality individual receiver functions that were used in the final stacks.

peak and some indications of multiples; therefore, we suspect that upper mantle heterogeneity may be affecting the character of the stacks.

5. Discussion

5.1. Transition Zone Thickness

Based on these findings and an interpretation of mantle transition zone thinning produced by an increase in temperature, we suggest that two distinct warm thermal anomalies may exist within the transition zone beneath West Antarctica caused by lower mantle sources, one beneath the Ruppert Coast in western Marie Byrd Land and one beneath the Bentley Subglacial Trench and Whitmore Mountains section of the West Antarctic Rift System (Figures 7c and 7d). However, it does not appear that a broad, region-wide, lower mantle upwelling exists beneath the whole West Antarctic Rift System [e.g., LeMasurier and Landis, 1996].

Beneath Marie Byrd Land, recent seismic tomography suggests the presence of slow material extending into and possibly through the mantle transition zone [Hansen *et al.*, 2014]. We do not find consistent and statistically significant evidence for transition zone thinning directly beneath the Executive Committee Range or eastern Marie Byrd Land; however, the regions of thinning beneath the Ruppert Coast/Ross Sea (210 ± 15 km) and the Bentley Subglacial Trench (225 ± 25 km) appear to occur near to or within portions of a low-velocity region at 500 km depth in recent tomography images from Hansen *et al.* [2014] (see Figure S2). The anomaly within the transition zone beneath the Bentley Subglacial Trench and southeastern end of the 2010–2012 ANET transect is broader, but exhibits less thinning than the anomaly along the Ruppert Coast. The location of thinning beneath the Bentley Subglacial Trench does not strongly correlate with the location of low velocity anomalies within the upper mantle in recent tomography models [Lloyd *et al.*, 2013; Hansen *et al.*, 2014], but may correlate with a deeper anomaly (~500 km) [Hansen *et al.*, 2014].

To provide comparison to other hot spot regions, in the following sections, we assume the range of possible transition zone thickness variations (δz) taken from our observations and confidence bounds and calculate the transition zone temperature anomaly for our two West Antarctic regions with thinned transition zone using:

$$\delta z = Z_{avg} + \delta T \times \frac{dz}{dP} \times \left[\left(\frac{dP}{dT} \right)_{660} - \left(\frac{dP}{dT} \right)_{410} \right], \quad (1)$$

with $(\frac{dp}{dT})_{410} = 3.1 \text{ MPa/}^\circ\text{K}$, $(\frac{dp}{dT})_{660} = -2.6 \text{ MPa/}^\circ\text{K}$, $\frac{dp}{dz} = 35 \text{ MPa/km}$, and $(Z_{avg}) = 250$ or 242 km average mantle transition zone thickness [Hellfrich, 2000; Lawrence and Shearer, 2006; Akaogi et al., 2007]. The Clapeyron slope for the anhydrous olivine-wadsleyite (410) transition is relatively well constrained [Hellfrich and Wood, 1996; Smyth and Frost, 2002]. However, the ringwoodite to perovskite (660) transition is not as well constrained; in the following paragraph, we consider a range of slopes for the 660 discontinuity and include that uncertainty in our expanded transition zone temperature anomaly estimates [Akaogi and Ito, 1993; Bina and Hellfrich, 1994; Irifune et al., 1998; Katsura et al., 2003; Fei et al., 2004; Litasov et al., 2005; Ye et al., 2014].

Beneath the Ruppert Coast near the eastern side of the Ross Ice Shelf, we infer a range of temperature anomalies of $\sim 100^\circ\text{K}$ – 340°K , although if we consider a range of values for the slope of the ringwoodite-perovskite transition, the resulting range of temperature anomaly expands to $\sim 95^\circ\text{K}$ – 550°K (see supporting information). This suggests, conservatively, that an anomaly of at least 100°K is present and that this thermal anomaly is on par with several other regions where transition zone-transiting mantle plumes have been proposed [Shen et al., 1996; Benoit et al., 2006; Cao et al., 2011; Benoit et al., 2013; Mulibo and Nyblade, 2013]. For the possible thermal anomaly beneath the Bentley Subglacial Trench, we estimate a ~ -50 to 300°K anomaly; and with some variation in the values of the ringwoodite-perovskite Clapeyron slope the anomaly expands to ~ -80 to 500°K . Due to the larger confidence bounds on the lower peak in these stacks and the differing values assumed for the global average thickness, the lower end of this range (negative) allows for the possibility that this is not a significant thermal anomaly.

The water content of the mantle transition zone is thought to impact the depth and the sharpness of phase transitions [Hellfrich, 2000]. The olivine-wadsleyite transition in an anhydrous Fo_{90} olivine should occur over $\sim 10 \text{ km}$ [Hellfrich and Wood, 1996; Smyth and Frost, 2002], but it has been found that the slope of the olivine-wadsleyite (410) transition in hydrous conditions may broaden, making it less seismically detectable, and occur at shallower depths, which would increase the thickness of the transition zone [Wood, 1995; Smyth and Frost, 2002]. When hydrous ringwoodite (1–3 wt % H_2O) is present in the bottom of the transition zone, the ringwoodite-perovskite transition may occur at deeper depths [Higo et al., 2001], although there is still some uncertainty regarding the water storage capacity of ringwoodite [Kohlstedt et al., 1996; Smyth et al., 2003]. Recent analyses from ringwoodite within ultradep diamonds suggest that, at least locally, 1 wt % H_2O is possible [Pearson et al., 2014], and observations consistent with a hydration influence on 660 and near-660 structures have been reported for downwelling regions of western North America [Schmandt et al., 2014].

5.2. Negative Receiver Function Peak Above 410

Several studies suggest that negative peaks located above the mantle transition zone are due to partial melt caused by upward flux of hydrated transition zone material [e.g., Revenaugh and Sipkin, 1994; Jasbinsek et al., 2010]; however, debate exists as to whether this peak is a global phenomenon or occurs only in the vicinity of upwelling mantle [Bercovici and Karato, 2003; Vinnik and Farra, 2007]. While the amplitude of the negative peak above the transition zone is the greatest beneath the WAIS Divide and Byrd Subglacial Basin, it is observed consistently throughout most of the study area (Figure 9b).

Bercovici and Karato [2003] originally envisioned partial melts to form due to upward displacement of transition zone material as a passive response to sinking slabs. This led to their proposal that this negative peak (or partial melt) would be identified nearly everywhere, except where hot mantle plumes exist (additional heat would allow the material to retain its water). Alternatively, Vinnik and Farra [2007] proposed that hydrous partial melt forms in the presence of mantle plumes, pointing to several hot spot locations where these negative peaks have been found. In areas where we interpret thinning of

the transition zone to be indicative of thermal upwellings, the negative anomaly is present, and in areas where the transition zone is not thinned, the anomaly is also present. Therefore, the nearly ubiquitous negative peak above the transition zone beneath the Byrd Subglacial Basin, Marie Byrd Land, Bentley Subglacial Trench, and Whitmore Mountains, does not fully support either of the existing hypotheses for where the negative peak does/does not occur [Bercovici and Karato, 2003; Vinnik and Farra, 2007].

In prior studies from other locations, observed negative receiver function peaks were located at 100 km or less above the transition zone [Revenaugh and Sipkin, 1994; Vinnik and Farra, 2007; Jasbinsek et al., 2010]; this feature should not be confused with the “X-discontinuity,” which is a reflector observed by SS and PP precursors at depths of 250–300 km that indicates seismically faster material, possibly related to eclogite within the crust of remnant subducted slabs [e.g., Revenaugh and Jordan, 1991; Deuss and Woodhouse, 2002; Bagley and Revenaugh, 2008; Schmerr et al., 2013]. Synthetic models based on receiver function results from the Colorado Plateau and Rio Grande Rift suggest that the low-velocity anomaly is best fit by a sharp, upper discontinuity and a ~20 km thick layer of low velocity material (~4.5% velocity reduction) that is underlain by a broad 410 discontinuity [Jasbinsek et al., 2010]. Throughout our study region, the low-velocity peak above the 410 was generally found at 50–60 km above the 410, with the exception of western Marie Byrd Land, where the 410 low velocity anomaly was found at ~100 km above the transition zone (330–350 km depth) (Figure 9a). Although this distance above the 410 is on par with some observations from Eastern China [Revenaugh and Sipkin, 1994], the interpretation that this is a gravitationally stable partial melt resting on top of the transition zone may be more difficult to reconcile [e.g., Bercovici and Karato, 2003]. The gravitational stability of a compressible melt above the 410 discontinuity is dependent upon the size of the melt layer and layer perturbations, and the water content of the melt; given a significant perturbation or a larger water content, melt layers may become unstable and rise into the upper mantle [Matsukage et al., 2005; Sakamaki et al., 2006; Youngs and Bercovici, 2009]. It is not clear whether a gravitational instability is a viable interpretation for the apparently shallow depths of the 410 low-velocity layer beneath the western Marie Byrd Land region; however, we note that such an upwelling has been proposed to explain observed low-velocity anomalies within the upper mantle beneath the Colorado Plateau [MacCarthy et al., 2014].

Our interpretation of the presence and strength of negative peaks above the West Antarctica mantle transition zone enforces prior work that suggests the mantle transition zone may be partly hydrated [Meier et al., 2009]. Furthermore, we note that the amplitude of this negative peak is the most prominent throughout the Byrd Subglacial Basin, Bentley Subglacial Trench, and Whitmore and Ellsworth Mountains; we suggest that the transition zone may be most hydrated in these regions.

5.3. Upper Mantle Slow Velocities

There is trade-off between estimated discontinuity depth and assumed Vp/Vs ratios in receiver function analysis. In areas where no thinning of the transition zone is detected, the depressed 410 is not caused by anomalous transition zone, but rather is caused by a Vp/Vs ratio within the upper mantle that is larger than the assumed global average model (Figure 6). In West Antarctica, compressional and shear wave tomography results indicate decreased upper mantle velocities [Ritzwoller et al., 2001; Danesi and Morelli, 2001; Sieminska et al., 2003; Morelli and Danesi, 2004; Heeszel, 2011; Lloyd et al., 2013; Hansen et al., 2014]. The apparent depression of the 410 above a transition zone of average thickness in this study requires that the Vp/Vs ratio in the upper mantle is greater than average, which simply requires a more pronounced decrease in Vs relative to Vp.

Previous research has focused on discerning relative effects of temperature on seismic velocity in an attempt to better understand how to interpret temperature from seismic velocity models; in the process, it has been found that due to effects of anelasticity, Vs is more responsive to temperature perturbations than Vp [Karato, 1993; Goes et al., 2000; Cammarano et al., 2003]. It follows that a larger than average Vp/Vs ratio is expected for warm regions of the upper mantle. Here observations of a depressed 410 with no accompanying transition zone thinning are most likely an indication that the upper mantle is thermally perturbed and thus seismically slower, and this agrees with results from compressional and shear velocity tomography (see Figure S1). Alternatively, significant amounts of partial melt present directly above the transition zone may also contribute to the apparent depression of

the 410 discontinuity, as partial melt should produce an even greater slowing of *S* waves relative to *P* waves.

With exception to the Central Transantarctic Mountains and the Ellsworth Mountains, the estimated depth of the 410 phase transition appears to be depressed beneath nearly all of West Antarctica (Figure 6). The 410 is most significantly depressed beneath the Eastern Marie Byrd Land, Executive Committee Range and the region beneath Thwaites and Pine Island Bay, and this corresponds closely with where upper mantle slow velocities are detected by recent seismic tomography results (Figure S1) [Hansen *et al.*, 2014]. Most of this same region (and further south toward the WAIS Divide and the Whitmore mountains) also is associated with prominent negative peaks above the 410 discontinuity. If, as suggested, this negative peak is produced by a region of water-induced partial melting above the mantle transition zone [i.e., Bercovici and Karato, 2003; Vinnik and Farra, 2007], then a reasonably thick layer of partial melt might also contribute toward the apparent, depressed 410 discontinuity.

5.4. 520 Discontinuity

Peaks consistent with the 520 discontinuity were visible in many of our common conversion point stacks in West Antarctica (Figure 8). Nodes where the greatest depression of the 410 exist tend to have weak or not-detectable 520 discontinuities. However, in many of our CCP stacks, full stack amplitude was greater than zero, but the peak was not statistically significant and was therefore not interpreted. Given the prominent negative peaks above the transition zone and results from Meier *et al.* [2009], we expect that the mantle transition zone is hydrated to some extent throughout the region. However, debate exists as to whether transition zone hydration would sharpen or decrease detectability of the 520 discontinuity [Inoue *et al.*, 1998; Yusa *et al.*, 2000; Weidner and Wang, 2000; Panero, 2010; Julià and Nyblade, 2013]. If we assume that partial melt above the transition zone is an indication that the transition zone below it is hydrated throughout, then the inconsistent detections of the 520 do not appear to be consistent with either interpretation for the effect of water on the wadsleyite-ringwoodite transition. However, temperature in conjunction with water may also affect the detectability of the 520 discontinuity—a sharp, easily detected 520 might be expected where the mantle transition zone is colder and more hydrated than average while a hotter and dryer transition zone may lessen our ability to detect the 520 [Inoue *et al.*, 1998; Xu *et al.*, 2008; Panero, 2010].

The 520 and the negative peak above the transition zone are the strongest near the WAIS Divide and Thwaites Glacier (Figure 8), where we estimate that the transition zone may be slightly thickened relative to the rest of the region. This would be consistent with the interpretation that a slightly colder and/or wetter than average transition zone may result in a sharper 520 detection; however the vertical uncertainties of mantle transition zone thickness in this region implies that no cool thermal anomaly may exist [Inoue *et al.*, 1998; Xu *et al.*, 2008; Panero, 2010]. We note that the 520 discontinuity was not detected or was weakly detected on some of the Executive Committee Range or Ruppert Coast stacks. Where it was detected beneath the Executive Committee Range, the amplitude of the 520 peak was small, but the thickness of the mantle transition zone in these regions was similar to the global average, and a prominent negative peak was detected above the transition zone (Figures 7 and 9). Although the stack from the Ruppert Coast region had a very slight peak where we would expect the 520 discontinuity, the amplitude was not resolvable above the uncertainty (Figure 7d). In this region, we have evidence for mantle transition zone thinning, but a low-velocity anomaly is detected above the transition zone (albeit at shallower depth) (Figures 7 and 9). Therefore, it appears that the hot and dry mantle transition zone interpretation does not quite fit this region, and we suspect that our ability to detect the 520 discontinuity may be partly a function of spatial resolution [Inoue *et al.*, 1998; Xu *et al.*, 2008; Panero, 2010].

5.5. Sub-660 Discontinuity (720)

The lower peak corresponding to the 660 discontinuity was notably complex beneath both of the regions where we interpret thermal mantle upwellings (multiple positive peaks, asymmetric, broad), and this may reveal increased temperatures at the base of the transition zone (Figures 7c and 7d). The complexity associated with the 660 discontinuity that we observed in West Antarctica did not include obvious sub-660 negative peaks as have been identified beneath parts of North America [Schmandt *et al.*, 2014]. Therefore, unlike

North America, we do not suspect very recent downwelling of hydrated material into the lower mantle or subsequent transient (gravitationally unstable) partial melts at the top of the lower mantle [Schmandt *et al.*, 2014].

It has been suggested that deeper positive peaks are indicative of a garnet majorite to perovskite transition in a hotter than average mantle transition zone [Simmons and Gurrola, 2000; Andrews and Deuss, 2008; Yu *et al.*, 2011], and if this is the case for West Antarctica, then the complexity of the 660 and the multiple positive peaks might be a secondary indication of a deep mantle upwelling. In this case, the thicker transition zone in the region surrounding the Ruppert Coast anomaly, for example, might possibly be interpreted as a result of the ringwoodite and garnet majorite transitions merging (shifting the 660 downward) as transition zone temperatures decrease and the olivine-normative and pyroxene-normative mineral phase transitions return to their average depth and character away from the hot center of the upwelling (Figure 7). However, as Schmandt *et al.* [2012] demonstrated, some of the complexity detected at the 660 discontinuity beneath Yellowstone can be explained as an effect of using a 1-D velocity model for the migration; therefore, as more data and more detailed regional tomographic models become available for this region, we expect that some of the observed complexity on the 660 found in our receiver function stacks may simplify (see discussion in supporting information).

5.6. Possible Lower Mantle Connectivity With Marie Byrd Land Volcanoes

As discussed, many of the Marie Byrd Land volcanoes bear some geochemical resemblance to ocean island basalts [LeMasurier, 1990], and several studies have suggested that a lower mantle plume source may explain this [e.g., LeMasurier and Landis, 1996; Panter *et al.*, 1997, 2000; Storey *et al.*, 1999; Kipf *et al.*, 2014]. The upper mantle beneath the region, and in particular, beneath eastern Marie Byrd Land and the Thwaites Glacier, appears to be thermally perturbed as evidenced by recent tomography studies and by our results showing a significantly depressed 410 (with no corresponding change in transition zone thickness) beneath this region [Heeszel, 2011; Lloyd *et al.*, 2013; Hansen *et al.*, 2014]. If the anomalies that we detect below the Ruppert Coast and the Bentley Subglacial Trench are connected to the prominent Marie Byrd Land upper mantle anomaly, then the geochemical characteristics of the volcanoes that suggest a lower mantle source may be related in this way to the seismic structure of the mantle.

6. Summary and Conclusions

We find that the 410 discontinuity is depressed relative to the global average throughout the study region in West Antarctica, and most strongly so beneath the Thwaites Glacier and Executive Committee Range where recent tomographic results image significantly decreased upper mantle velocities. This suggests that the apparent depression of the 410 results from velocity effects within the upper mantle and does not represent actual topography of the olivine-wadsleyite transition. The mantle transition zone thickness throughout most of the region is comparable to the global average (and consistent with earlier studies beneath the Erebus hot spot). However, thinner than average transition zone is found beneath the Bentley Subglacial Trench and Whitmore Mountains, and beneath the Ruppert Coast on the eastern side of the Ross Ice Shelf. The 520 discontinuity is detected beneath much of the study region and has the highest stack amplitudes beneath the WAIS Divide and Thwaites Glacier. A negative peak consistent with a low velocity layer above the 410 is detected above the transition zone throughout most of the region, and its amplitude is the strongest beneath the Byrd Subglacial Basin and the WAIS Divide. Lastly, we observed complicated peaks from the (sub-660) base of the transition zone in regions where transition zone thinning is present, although some of the characteristics of these features may arise from unaccounted-for 3-D velocity effects.

We conclude that the evidence from P-receiver functions suggests two distinct thermal upwellings beneath West Antarctica: one beneath the Ruppert Coast and another beneath the Bentley Subglacial Trench. These regions may be connected to the pronounced upper mantle thermal anomalies beneath the Executive Committee Range of Marie Byrd Land and Thwaites Glacier, which supports geochemical evidence for a mantle plume influence on Marie Byrd Land volcanism. We further propose that the transition zone shows indications of being partially hydrated. The source of this hydration may be a remnant of subduction off the coast of West Antarctica prior to the Cretaceous.

Acknowledgments

Seismic instrumentation was provided and supported by the Incorporated Research Institutions for Seismology (IRIS) through the PASSCAL Instrument Center at New Mexico Tech. We gratefully acknowledge scientific and field support provided by engineers from IRIS/PASSCAL Polar Programs, pilots from Kenn Borek Air Ltd. and PHI, Inc., mountaineers M. Roberts, J. Roberts, M. Whetu, and R. McBrearty, and numerous scientists and students who participated as part of field crews. We thank N. Accardo, R. Brazier, J. Chaput, P. Crotwell, E. Day, S. Hansen, D. Heeszel, M. Kachingwe, A. Lloyd, A. Lough, A. Muto, J. O'Donnell, C. Ramirez, A. Raveloson, A. Reusch, and P. Winberry for scientific discussion and technical assistance that improved this paper. This work has been supported by NSF Polar Programs (grant 0632136, 0632185, 0632209, 0632330, 0632239, 0652322, 0632335, 1246666, 1246712, 1246776, 1247518, 1249513, 1249631, and 1419268) and NSF Earth Sciences Postdoctoral Fellowship (grant 1349684). Seismic data for the Antarctic-POLENET project (network code: YT) are available through the IRIS Data Management Center (<http://www.iris.edu/mda>) and were accessed using the Standing Order for Data (SOD) request software (<http://www.seis.sc.edu/sod/>). Data for the figures in the paper are in the supporting information. If you would like access to other results data, contact corresponding author E. L. Emry at ele11@psu.edu. Maps were created using the Generic Mapping Tools (GMT) software (<http://www.soest.hawaii.edu/gmt/>).

References

- Abt, D. L., K. M. Fischer, S. W. French, H. A. Ford, H. Yuan, and B. Romanowicz (2010), North American lithospheric discontinuity structure imaged by Ps and Sp receiver functions, *J. Geophys. Res.*, 115, B09301, doi:10.1029/2009JB006914.
- Akaogi, M., and E. Ito (1993), Refinement of enthalpy measurement of Mg_2SiO_4 perovskite and negative pressure-temperature slopes for perovskite-forming reactions, *Geophys. Res. Lett.*, 20(17), 1839–1842, doi: 10.1029/93GL01265.
- Akaogi, M., H. Takayama, H. Kojitani, H. Kawaji, and T. Atake (2007), Low-temperature heat capacities, entropies and enthalpies of Mg_2SiO_4 polymorphs, and α - β - γ and post-spinel phase relations at high pressure, *Phys. Chem. Miner.*, 34, 169–183, doi:10.1007/s00269-006-0137-3.
- Alley, R. B., and C. R. Bentley (1988), Ice-core analysis on the Siple Coast of West Antarctica, *Ann. Glaciol.*, 11, 1–7.
- Andrews, J., and A. Deuss (2008), Detailed nature of the 660 km region of the mantle from global receiver function data, *J. Geophys. Res.*, 113, B06304, doi:10.1029/2007JB005111.
- Anthony, R. E., R. C. Aster, D. Wiens, A. Nyblade, S. Anandakrishnan, J. P. Winberry, T. Wilson, and C. Rowe (2015), The seismic noise environment of Antarctica, *Seismol. Res. Lett.*, 86(1), doi:10.1785/0220140109.
- Bagley, B., and J. Revenaugh (2008), Upper mantle seismic shear discontinuities of the Pacific, *J. Geophys. Res.*, 113, B12301, doi:10.1029/2008JB005692.
- Behrendt, J. C. (2012), The aeromagnetic method as a tool to identify Cenozoic magmatism in the West Antarctic Rift System beneath the West Antarctic Ice Sheet—A review; Thiel subglacial volcano as a possible source of the ash layer in the WAISCORE, *Tectonophysics*, 585, 124–136.
- Behrendt, J. C., W. E. LeMasurier, A. K. Cooper, F. Tessensohn, A. Tréhu, and D. Damaske (1991), Geophysical studies of the West Antarctic Rift System, *Tectonics*, 10(6), 1257–1273, doi:10.1029/91TC00868.
- Benoit, M. H., A. A. Nyblade, T. J. Owens, and G. Stuart (2006), Mantle transition zone structure and upper mantle S velocity variations beneath Ethiopia: Evidence for a broad, deep-seated thermal anomaly, *Geochim. Geophys. Geosyst.*, 7, Q11013, doi:10.1029/2006GC001398.
- Benoit, M. H., M. D. Long, and S. D. King (2013), Anomalously thin transition zone and apparently isotropic upper mantle beneath Bermuda: Evidence for upwelling, *Geochim. Geophys. Geosyst.*, 14, 4282–4291, doi:10.1002/ggge.20277.
- Bercovici, D., and S. Karato (2003), Whole-mantle convection and the transition-zone water filter, *Nature*, 425, 39–44, doi: 10.1038/nature01918.
- Bina, C. R., and G. Hellfrich (1994), Phase transition Clapeyron slopes and transition zone seismic discontinuity topography, *J. Geophys. Res.*, 99(B8), 15,853–15,860, doi: 10.1029/94JB00462.
- Blankenship, D. D., R. E. Bell, S. M. Hodge, J. M. Brozena, J. C. Behrendt, and C. A. Finn (1993), Active volcanism beneath the West Antarctic ice sheet and implications for ice-sheet stability, *Nature*, 361, 526–529, doi: 10.1038/361526a0.
- Cammarano, F., S. Goes, P. Vacher, and D. Giardini (2003), Inferring upper-mantle temperatures from seismic velocities, *Phys. Earth Planet. Inter.*, 138, 197–222, doi:10.1016/S0031-9201(03)00156-0.
- Cao, Q., R. D. van der Hilst, M. V. de Hoop, and S.-H. Shim (2011), Seismic imaging of transition zone discontinuities suggests hot mantle west of Hawaii, *Science*, 332, 1068–1071, doi:10.1126/science.1202731.
- Chevrot, S., L. Vinnik, and J.-P. Montagner (1999), Global-scale analysis of the mantle Pds phases, *J. Geophys. Res.*, 104(B9), 20,203–20,219, doi: 10.1029/1999JB900087.
- Clow, G. D., K. M. Cuffey, and E. D. Waddington (2012), High heat-flow beneath the central portion of the West Antarctic Ice Sheet, Abstract C31A-0577 presented at 2012 Fall Meeting, AGU, San Francisco, Calif., 3–7 Dec.
- Crotwell, H. P., T. J. Owens, and J. Ritsema (1999), The TauP toolkit: Flexible seismic travel-time and ray-path utilities, *Seismol. Res. Lett.*, 70, 154–160, doi: 10.1785/gssrl.70.2.154.
- Dalziel, I. W. D. (1992), Antarctica: A tale of two supercontinents?, *Annu. Rev. Earth Planet. Sci.*, 20, 501–526, doi: 10.1146/annurev.ea.20.050192.002441.
- Dalziel, I. W. D., and D. H. Elliot (1982), West Antarctica: Problem child of Gondwanaland, *Tectonics*, 1(1), 3–19, doi:10.1029/TC001i001p00003.
- Danesi, S., and A. Morelli (2001), Structure of the upper mantle under the Antarctic Plate from surface wave tomography, *Geophys. Res. Lett.*, 28(23), 4395–4398, doi: 10.1029/2001GL013431.
- Deuss, A., and J. Woodhouse (2001), Seismic observations of splitting of the mid-transition zone discontinuity in Earth's mantle, *Science*, 294, 354–357, doi:10.1126/science.1063524.
- Deuss, A., and J. H. Woodhouse (2002), A systematic search for mantle discontinuities using SS-preursors, *Geophys. Res. Lett.*, 29(8), 1249, doi:10.1029/2002GL014768.
- Dueker, K. G., and A. F. Sheehan (1997), Mantle discontinuity structure from midpoint stacks of converted P to S waves across the Yellowstone hotspot track, *J. Geophys. Res.*, 102(B4), 8313–8327, doi: 10.1029/96JB03857.
- Efron, B., and R. Tibshirani (1991), Statistical data analysis in the computer age, *Science*, 253(5018), 390–395, doi: 10.1126/science.253.5018.390.
- Fei, Y., J. Van Orman, J. Li, W. van Westrenen, C. Sanloup, W. Minarik, K. Hirose, T. Komabayashi, M. Walter, and K. Funakoshi (2004), Experimentally determined postspinel transformation boundary in Mg_2SiO_4 using MgO as an internal pressure standard and its geophysical implications, *J. Geophys. Res.*, 109, B02305, doi:10.1029/2003JB002562.
- Finn, C. A., R. D. Müller, and K. S. Panter (2005), A Cenozoic diffuse alkaline magmatic province (DAMP) in the southwest Pacific without rift or plume origin, *Geochim. Geophys. Geosyst.*, 6, Q02005, doi:10.1029/2004GC000723.
- Fretwell, P., et al. (2013), Bedmap2: Improved ice bed, surface and thickness datasets for Antarctica, *Cryosphere*, 7, 375–393, doi: 10.5194/tc-7-375-2013.
- Goes, S., R. Govers, and P. Vacher (2000), Shallow mantle temperatures under Europe from P and S wave tomography, *J. Geophys. Res.*, 105(B5), 11,153–11,169, doi: 10.1029/1999JB900300.
- Grunow, A. M., D. V. Kent, and I. W. D. Dalziel (1991), New paleomagnetic data from Thurston Island: Implications for the tectonics of West Antarctica and Weddell Sea opening, *J. Geophys. Res.*, 96(B11), 17,935–17,954, doi: 10.1029/91JB01507.
- Hansen, S. E., and A. A. Nyblade (2013), The deep seismic structure of the Ethiopia/Afar hotspot and the African superplume, *Geophys. J. Int.*, 194, 118–124, doi: 10.1093/gji/gjt116.
- Hansen, S. E., J. H. Graw, L. M. Kenyon, A. A. Nyblade, D. A. Wiens, R. C. Aster, A. D. Huerta, S. Anandakrishnan, and T. Wilson (2014), Imaging the Antarctic mantle using adaptively parameterized P-wave tomography: Evidence for heterogeneous structure beneath West Antarctica, *Earth Planet. Sci. Lett.*, 408, 66–78, doi:10.1016/j.epsl.2014.09.043.
- Heeszel, D. (2011), Surface wave derived shear velocity structure of the Gamburtsev Subglacial Mountains, Transantarctic Mountains, and West Antarctica and shallow seismicity of the Mariana and Tonga Subduction Zones, PhD thesis, 172 pp., Dep. of Earth and Planet. Sci., Washington Univ. in St. Louis, St. Louis, Mo.
- Hellfrich, G. (2000), Topography of the transition zone seismic discontinuities, *Rev. Geophys.*, 38(1), 141–158, doi: 10.1029/1999RG000060.
- Hellfrich, G. R., and B. J. Wood (1996), 410 km discontinuity sharpness and the form of the olivine α - β phase diagram: Resolution of apparent seismic contradictions, *Geophys. J. Int.*, 126, F7–F12, doi:10.1111/j.1365-246X.1996.tb05292.x.

- Higo, Y., T. Inoue, T. Irifune, and H. Yurimoto (2001), Effect of water on the spinel-postspinel transformation in Mg_2SiO_4 , *Geophys. Res. Lett.*, 28(18), 3505–3508, doi: 10.1029/2001GL013194.
- Inoue, T., D. J. Weidner, P. A. Northrup, and J. B. Parise (1998), Elastic properties of hydrous ringwoodite (γ -phase) in Mg_2SiO_4 , *Earth Planet. Sci. Lett.*, 160, 107–113, doi: 10.1016/S0016-821X(98)00077-6.
- Irifune, T., et al. (1998), The postspinel phase boundary in Mg_2SiO_4 determined by in situ x-ray diffraction, *Science*, 279, 1698–1700, doi: 10.1126/science.279.5357.1698.
- Ita, J., and L. Stixrude (1992), Petrology, elasticity, and composition of the mantle transition zone, *J. Geophys. Res.*, 97(B5), 6849–6866, doi: 10.1029/92JB00068.
- Jasbinsek, J. J., K. Dueker, and S. M. Hansen (2010), Characterizing the 410 Km discontinuity low-velocity layer beneath the La Ristra array in the North American Southwest, *Geochem. Geophys. Geosyst.*, 11, Q03008, doi: 10.1029/2009GC002836.
- Jordan, T. A., F. Ferraccioli, D. G. Vaughan, J. W. Holt, H. Corr, D. D. Blankenship, and T. M. Diehl (2010), Aerogravity evidence for major crustal thinning under the Pine Island Glacier region (West Antarctica), *Geol. Soc. Am. Bull.*, 122(5/6), 714–726, doi: 10.1130/B26417.1.
- Julia, J., and A. A. Nyblade (2013), Probing the upper mantle transition zone under Africa with P520s conversions: Implications for temperature and composition, *Earth Planet. Sci. Lett.*, 368, 151–162, doi: 10.1016/j.epsl.2013.02.021.
- Karato, S. (1993), Importance of anelasticity in the interpretation of seismic tomography, *Geophys. Res. Lett.*, 20(15), 1623–1626, doi: 10.1029/93GL01767.
- Katsura, T., et al. (2003), Post-spinel transition in Mg_2SiO_4 determined by high P-T in situ X-ray diffractometry, *Phys. Earth Planet. Inter.*, 136, 11–24, doi: 10.1016/S0031-9201(03)00019-0.
- Kennett, B. L. N., E. R. Engdahl, and R. Buland (1995), Constraints on seismic velocities in the earth from travel times, *Geophys. J. Int.*, 122, 108–124, doi: 10.1111/j.1365-246X.1995.tb03540.x.
- Kipf, A., F. Hauff, R. Werner, K. Gohl, P. van den Bogaard, K. Hoernle, D. Maicher, and A. Klügel (2014), Seamounts off the West Antarctic margin: A case for non-hotspot driven intraplate volcanism, *Gondwana Res.*, 25(4), 1660–1679, doi: 10.1016/j.gr.2013.06.013.
- Kohlstedt, D. L., H. Keppler, and D. C. Rubie (1996), Solubility of water in the α , β , and γ phases of $(Mg,Fe)_2SiO_4$, *Contrib. Mineral. Petrol.*, 123, 345–357, doi: 10.1007/s004100050161.
- Langston, C. A. (1979), Structure under Mount Rainier, Washington, inferred from teleseismic body waves, *J. Geophys. Res.*, 84(B9), 4749–4762, doi: 10.1029/JB084iB09p04749.
- Lawrence, J. F., and P. M. Shearer (2006), A global study of transition zone thickness using receiver functions, *J. Geophys. Res.*, 111, B06307, doi: 10.1029/2005JB003973.
- Lawrence, J. F., D. A. Wiens, A. A. Nyblade, S. Anandakrishnan, P. J. Shore, and D. Voigt (2006), Upper mantle thermal variations beneath the Transantarctic Mountains inferred from teleseismic S-wave attenuation, *Geophys. Res. Lett.*, 33, L03303, doi: 10.1029/2005GL024516.
- LeMasurier, W. E. (1990), Marie Byrd Land summary, in *Volcanoes of the Antarctic Plate and Southern Ocean, Antarctic Res. Ser.*, vol. 48, edited by W. E. LeMasurier and J. W. Thomson, pp. 147–163, AGU, Washington, D. C.
- LeMasurier, W. E., and C. A. Landis (1996), Mantle-plume activity recorded by low-relief erosion surfaces in West Antarctica and New Zealand, *Geol. Soc. Am. Bull.*, 108(11), 1450–1466, doi: 10.1130/0016-7606(1996)108<1450:MPARBL>2.3.CO;2.
- LeMasurier, W. E., and D. C. Rex (1989), Evolution of linear volcanic ranges in Marie Byrd Land, West Antarctica, *J. Geophys. Res.*, 94(B6), 7223–7236, doi: 10.1029/JB094iB06p07223.
- Ligorría, J. P., and C. J. Ammon (1999), Iterative deconvolution and receiver-function estimation, *Bull. Seismol. Soc. Am.*, 89(5), 1395–1400.
- Litasov, K., E. Ohtani, A. Sano, A. Suzuki, and K. Funakoshi (2005), In situ X-ray diffraction study of post-spinel transformation in a peridotite mantle: Implication for the 660-km discontinuity, *Earth Planet. Sci. Lett.*, 238, 311–328, doi: 10.1016/j.epsl.2005.08.001.
- Lloyd, A. J., D. A. Wiens, A. Nyblade, S. L. Anandakrishnan, R. C. Aster, A. D. Huerta, T. J. Wilson, and P. J. Shore (2013), Tomographic evidence for recent extension in the Bentley Subglacial Trench and a hotspot beneath Marie Byrd Land, Abstract T12A-04 presented at 2013 Fall Meeting, AGU, San Francisco, Calif.
- Lough, A. C., D. A. Wiens, C. G. Barcheck, S. Anandakrishnan, R. C. Aster, D. D. Blankenship, A. D. Huerta, A. Nyblade, D. A. Young, and T. J. Wilson (2013), Seismic detection of an active subglacial magmatic complex in Marie Byrd Land, Antarctica, *Nat. Geo.*, 6, 1031–1035, doi: 10.1038/ngeo1992.
- MacCarthy, J. K., R. C. Aster, K. Dueker, S. Hansen, B. Schmandt, and K. Karlstrom (2014), Seismic tomography of the Colorado Rocky Mountains upper mantle from CREST: Lithosphere-asthenosphere interactions and mantle support of topography, *Earth Planet. Sci. Lett.*, 402, 107–119, doi: 10.1016/j.epsl.2014.03.063.
- Matsukage, K. N., Z. Jing, and S. Karato (2005), Density of hydrous silicate melt at the conditions of Earth's deep upper mantle, *Nature*, 438, 488–491, doi: 10.1038/nature04241.
- Meier, U., J. Trampert, and A. Curtis (2009), Global variations of temperature and water content in the mantle transition zone from higher mode surface waves, *Earth Planet. Sci. Lett.*, 282, 91–101, doi: 10.1016/j.epsl.2009.03.004.
- Morelli, A., and S. Danesi (2004), Seismological imaging of the Antarctic continental lithosphere: A review, *Global Planet. Change*, 42, 155–165, doi: 10.1016/j.gloplacha.2003.12.005.
- Mulibio, G. D., and A. A. Nyblade (2013), Mantle transition zone thinning beneath eastern Africa: Evidence for a whole-mantle superplume structure, *Geophys. Res. Lett.*, 40, 3562–3566, doi: 10.1002/grl.50694.
- Owens, T. J., A. A. Nyblade, H. Gurrola, and C. A. Langston (2000), Mantle transition zone structure beneath Tanzania, East Africa, *Geophys. Res. Lett.*, 27(6), 827–830, doi: 10.1029/1999GL005429.
- Panero, W. R. (2010), First principles determination of the structure and elasticity of hydrous ringwoodite, *J. Geophys. Res.*, 115, B03203, doi: 10.1029/2008JB006282.
- Panter, K. S., P. R. Kyle, and J. L. Smellie (1997), Petrogenesis of a phonolite-trachyte succession at Mount Sidley, Marie Byrd Land, Antarctica, *J. Petrol.*, 38(9), 1225–1253, doi: 10.1093/petroj/38.9.1225.
- Panter, K. S., S. R. Hart, P. Kyle, J. Bluszczan, and T. Welch (2000), Geochemistry of Late Cenozoic basalts from the Crary Mountains: Characterization of mantle sources in Marie Byrd Land, Antarctica, *Chem. Geogr.*, 165, 215–241, doi: 10.1016/S0009-2541(99)00171-0.
- Pearson, D. G., et al. (2014), Hydrous mantle transition zone indicated by ringwoodite included within diamond, *Nature*, 507, 221–224, doi: 10.1038/nature13080.
- Reusch, A. M., A. A. Nyblade, M. H. Benoit, D. A. Wiens, S. Anandakrishnan, D. Voigt, and P. J. Shore (2008), Mantle transition zone thickness beneath Ross Island, the Transantarctic Mountain and East Antarctica, *Geophys. Res. Lett.*, 35, L12301, doi: 10.1029/2008GL033873.
- Revenaugh, J., and T. H. Jordan (1991), Mantle layering from ScS reverberations: 3. The upper mantle, *J. Geophys. Res.*, 96(B12), 19,781–19,810, doi: 10.1029/91JB01487.
- Revenaugh, J., and S. A. Sipkin (1994), Seismic evidence for silicate melt atop the 410-km mantle discontinuity, *Nature*, 369, 474–476, doi: 10.1038/369474a0.

- Ritzwoller, M. H., N. M. Shapiro, A. L. Levshin, and G. M. Leahy (2001), Crustal and upper mantle structure beneath Antarctica and surrounding oceans, *J. Geophys. Res.*, 106(12), 30,645–30,670, doi: 10.1029/2001JB000179.
- Saikia, A., D. J. Frost, and D. C. Rubie (2008), Splitting of the 520-kilometer seismic discontinuity and chemical heterogeneity in the mantle, *Science*, 319, 1515–1518, doi: 10.1126/science.1152818.
- Sakamaki, T., A. Suzuki, and E. Ohtani (2006), Stability of hydrous melt at the base of the Earth's upper mantle, *Nature*, 439, 192–194, doi: 10.1038/nature04352.
- Schmandt, B., K. Dueker, E. Humphreys, and S. Hansen (2012), Hot mantle upwelling across the 660 beneath Yellowstone, *Earth Planet. Sci. Lett.*, 331–332, 224–236, doi: 10.1016/j.epsl.2012.03.025.
- Schmandt, B., S. Jacobsen, T. Becker, Z. Liu, and K. Dueker (2014), Dehydration melting at the top of the lower mantle, *Science*, 344(6189), 1265–1268, doi: 10.1126/science.1253358.
- Schmerr, N. C., B. M. Kelly, and M. S. Thorne (2013), Broadband array observations of the 300 km seismic discontinuity, *Geophys. Res. Lett.*, 40, 841–846, doi: 10.1002/grl.50257.
- Shearer, P. M. (1991), Constraints on upper mantle discontinuities from observations of long-period reflected and converted phases, *J. Geophys. Res.*, 96(B11), 18,147–18,182, doi: 10.1029/91JB01592.
- Shen, Y., S. C. Solomon, I. Th. Bjarnason, and G. M. Purdy (1996), Hot mantle transition zone beneath Iceland and the adjacent Mid-Atlantic Ridge inferred from P-to-S conversions at the 410- and 660-km discontinuities, *Geophys. Res. Lett.*, 23(24), 3527–3530, doi: 10.1029/96GL03371.
- Sieminski, A., E. Debayle, and J.-J. Lévéque (2003), Seismic evidence for deep low-velocity anomalies in the transition zone beneath West Antarctica, *Earth Planet. Sci. Lett.*, 216, 645–661, doi: 10.1016/S0012-821X(03)00518-1.
- Simmons, N. A., and H. Gurrola (2000), Multiple seismic discontinuities near the base of the transition zone in the Earth's mantle, *Nature*, 405, 559–562, doi: 10.1038/35014589.
- Smyth, J. R., and D. J. Frost (2002), The effect of water on the 410-km discontinuity: An experimental study, *Geophys. Res. Lett.*, 29(10), 1485, doi: 10.1029/2001GL014418.
- Smyth, J. R., C. M. Holl, D. J. Frost, S. D. Jacobsen, F. Langenhorst, and C. A. McCammon (2003), Structural systematics of hydrous ringwoodite and water in Earth's interior, *Am. Mineral.*, 88, 1402–1407.
- Storey, B. C., P. T. Leat, S. D. Weaver, R. J. Pankhurst, J. D. Bradshaw, and S. Kelley (1999), Mantle plumes and Antarctica—New Zealand rifting: Evidence from mid-Cretaceous mafic dykes, *J. Geol. Soc. London*, 156, 659–671, doi: 10.1144/gsjgs.156.4.0659.
- Stump, E., and P. G. Fitzgerald (1992), Episodic uplift of the Transantarctic Mountains, *Geology*, 20, 161–164, doi: 10.1130/0091-7613(1992)020<0161:EUOTTM>2.3.CO;2.
- van Wijk, J., W. S. Baldridge, J. van Hunen, S. Goes, R. Aster, D. Coblenz, S. Grand, and J. Ni (2010), Small scale convection at the edge of the Colorado Plateau: Implications for topography, magmatism, and evolution of Proterozoic lithosphere, *Geology*, 38, 611–614, doi: 10.1130/G31031.1.
- Vinnik, L., and V. Farra (2007), Low S velocity atop the 410-km discontinuity and mantle plumes, *Earth Planet. Sci. Lett.*, 262, 398–412, doi: 10.1016/j.epsl.2007.07.051.
- Watson, T., A. Nyblade, D. A. Wiens, S. Anandakrishnan, M. Benoit, P. J. Shore, D. Voigt, and J. VanDecar (2006), P and S velocity structure of the upper mantle beneath the Transantarctic Mountains, East Antarctic craton, and Ross Sea from travel time tomography, *Geochem. Geophys. Geosyst.*, 7, Q07005, doi: 10.1029/2005GC001238.
- Weidner, D. J., and Y. Wang (2000), Phase transformations: Implication for mantle structure, in *Earth's Deep Interior: Mineral Physics and Tomography From the Atomic to the Global Scale*, *Geophys. Monogr. Ser.*, vol. 117, edited by S. Karato et al., pp. 215–235, AGU, Washington, D. C., doi: 10.1029/GM117p0215.
- Winberry, J. P., and S. Anandakrishnan (2003), Seismicity and neotectonics of West Antarctica, *Geophys. Res. Lett.*, 30(18), 1931, doi: 10.1029/2003GL018001.
- Wood, B. J. (1995), The effect of H₂O on the 410-kilometer seismic discontinuity, *Science*, 268(5207), 74–76, doi: 10.1126/science.268.5207.74.
- Xu, W., C. Lithgow-Bertelloni, L. Stixrude, and J. Ritsema (2008), The effect of bulk composition and temperature on mantle seismic structure, *Earth Planet. Sci. Lett.*, 275, 70–79, doi: 10.1016/j.epsl.2008.08.012.
- Ye, Y., C. Gu, S.-H. Shim, Y. Meng, and V. Prakapenka (2014), The postspinel boundary in pyrolytic compositions determined in the laser-heated diamond anvil cell, *Geophys. Res. Lett.*, 41, 3833–3841, doi: 10.1002/2014GL060060.
- Youngs, B. A. R., and D. Bercovici (2009), Stability of a compressible hydrous melt layer above the transition zone, *Earth Planet. Sci. Lett.*, 278, 78–86, doi: 10.1016/j.epsl.2008.11.024.
- Yu, Y. G., R. M. Wentzcovitch, V. L. Vinograd, and R. J. Angel (2011), Thermodynamic properties of MgSiO₃ majorite and phase transitions near 660 km depth in MgSiO₃ and Mg₂SiO₄: A first principles study, *J. Geophys. Res.*, 116, B02208, doi: 10.1029/2010JB007912.
- Yusa, H., T. Inoue, and Y. Ohishi (2000), Isothermal compressibility of hydrous ringwoodite and its relation to the mantle discontinuities, *Geophys. Res. Lett.*, 27(3), 413–416, doi: 10.1029/1999GL011032.